Intrinsic radial breathing oscillation in suspended single-walled carbon nanotubes

Kaihui Liu,[1,3] Wenlong Wang,[3] Muhong Wu,[3] Fajun Xiao,[1] Xiaoping Hong,[1] Shaul Aloni,[2] Xuedong Bai,[3] Enge Wang,[4,*] and Feng Wang[1,2,†]

[1]*Department of Physics, University of California at Berkeley, Berkeley, California 94720, USA*

[2]*The Molecular Foundry, Lawrence Berkeley National Laboratory, Berkeley, California 94720, USA*

[3]*Institute of Physics, Chinese Academy of Sciences, Beijing 100190, China*

[4]*International Center for Quantum Materials, School of Physics, Peking University, Beijing 100871, China*

(Received 17 January 2011; published 22 March 2011)

Radial breathing mode (RBM) oscillation is the most characteristic vibration mode in carbon nanotubes. Here we investigate the intrinsic behavior of RBM oscillations of structurally defined single-walled carbon nanotubes (SWNTs) by combining Raman-scattering and electron-diffraction techniques on the same suspended nanotubes. The independent determination of RBM frequencies and nanotube structures allows us to establish conclusively the perfect linear relation between RBM frequencies and inverse nanotube diameters, which has been long speculated to hold in pristine SWNTs. Understanding the intrinsic diameter dependence of SWNT RBM oscillation not only is crucial for reliable Raman characterization of carbon nanotubes, but also enables quantitative probing of SWNT-environment interactions through the RBM oscillation frequency shift.

DOI: 10.1103/PhysRevB.83.113404 PACS number(s): 78.67.Ch, 61.46.Np, 73.22.−f, 78.30.Na

I. INTRODUCTION

Single-walled carbon nanotubes (SWNTs) are one-dimensional (1D) tubular form of graphitic structures.[1,2] A signature of the 1D nanotube is the characteristic radial breathing mode (RBM) oscillation.[3] Since their observation in early Raman studies, RBM oscillations have been extensively investigated. The RBM frequency (ω_{RBM}) exhibits strong diameter (d) dependence, and it is widely used in characterizing SWNT diameter distributions.[4,5] The RBM oscillation has also guided spectroscopic studies of SWNTs and enabled structural assignment of optical transitions in SWNTs.[6–11] In spite of their obvious importance, however, the intrinsic behavior of RBM oscillations has not been firmly established. Theoretically RBM frequency is predicted to scale perfectly with the inverse of SWNT diameter.[12–14] Experimentally such ideal scaling was rarely observed. Instead the RBM frequency was described empirically by $\omega_{\mathrm{RBM}} = A/d + B$, and the values of A and B vary significantly in different studies. For nanotubes on substrates or in surfactants, the finite values of B were attributed to environmental effects.[7–10] Recently a zero value of B was inferred from Raman excitation spectroscopy of weakly bundled "supergrowth" nanotube arrays using a sophisticated and rather involved analysis.[15] It will be highly desirable to have a direct test of this relation by measuring RBM oscillation of individual clean nanotubes with unambiguous chirality identification.

Here we investigate quantitatively the intrinsic behavior of RBM oscillations in chirality resolved, pristine suspended SWNTs. We measured RBM oscillations in more than 25 structurally defined SWNTs with wide diameter distribution by combining electron-diffraction[16–18] and Raman-scattering[19–21] techniques on the same suspended nanotubes. Our suspended SWNTs are clean and isolated from external perturbations. We demonstrate that RBM oscillation frequency does scale linearly with the inverse of diameter in these pristine SWNTs, and we determine the scaling constant with an unprecedented precision. Understanding the intrinsic behavior of RBM oscillation not only is critical for spectral characterization of pristine SWNTs, but also opens up new opportunities for probing nanoscale coupling between SWNTs and other structures. For example, it allows quantitative examination of nanotube-environment interactions through small RBM frequency shifts induced by such interactions.

II. EXPERIMENT AND RESULTS

Our experimental setup for combined electron-diffraction and Raman-scattering techniques on the same nanotubes is illustrated in Fig. 1(a). The samples consist of ultralong SWNTs suspended over open slits. The slits (20–50 μm wide and 0.4 mm long) were fabricated on the Si_3N_4/Si substrate using standard photolithography and wet etching processes.[22] Millimeter-long isolated SWNTs were grown across the slit by chemical vapor deposition (CVD) method at 900 °C for 1 h.[23–25] We used methane in hydrogen ($CH_4 : H_2 = 1 : 2$) as feedstock and an ultrathin film (∼0.25 nm) of Fe as the catalyst. This growth condition yields extremely clean suspended nanotubes free of amorphous carbon and other adsorbates, as can be seen in the scanning electron micrograph [Fig. 1(b)] and high-resolution transmission electron micrograph [Fig. 1(c)] of our samples. These clean suspended nanotubes are critical for investigating intrinsic SWNT behavior.

We performed the electron-diffraction measurements on suspended SWNTs in a JEOL 2100 transmission electron microscope (TEM) operated at 80 keV. A parallel 20-nm-diameter electron beam was used to illuminate the sample, and no radiation damage was observed during the exposure.[26] The diffraction patterns were recorded by a high-resolution (2048 × 2048 pixels) two-dimensional charge-coupled device (CCD) array, and analyzed by recently developed routine procedures to reliably identify the SWNT chiral indices (n,m).[16–18] For a SWNT with chiral indices (n,m), the diameter is precisely known from the nanotube geometry and is described as $d = a_{c-c}\sqrt{3(n^2 + nm + m^2)}/\pi$, where $a_{c-c} = 0.142$ nm is the carbon-carbon bond length.

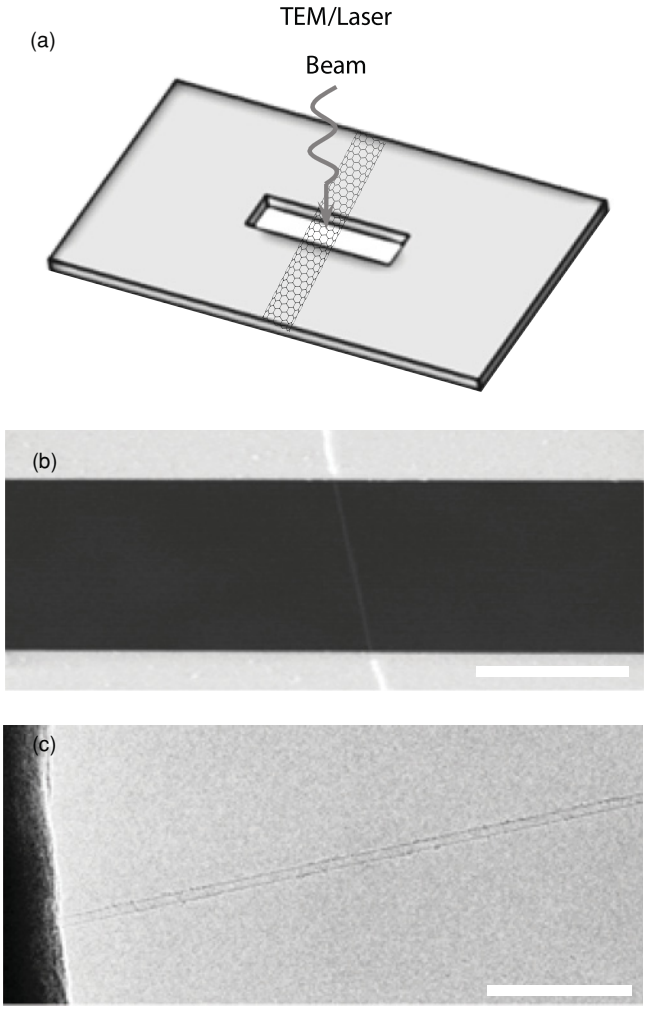

FIG. 1. (a) Schematic illustration for combined TEM electron-diffraction and Raman-scattering techniques on the same suspended nanotubes. (b) Scanning electron micrograph of a SWNT suspended across an open slit on the Si_3N_4/Si substrate. (c) High-resolution transmission electron micrograph of a SWNT. It is seen to be a single-walled character with clean surface. Scale bars in (b) and (c) are 20 μm and 20 nm, respectively.

Our suspended nanotubes are controlled to be well separated from each other, with an average separation over 20 μm (Fig. S1 in supplemental information[29]).[27] Using the slit edges as the spatial marker, we can reliably relocate any given nanotube in both TEM and optical microscopy setup. This allows us to perform micro-Raman measurements on the same SWNT characterized by TEM diffraction. We collected micro-Raman spectra in a backscattering geometry and used 1.96- or 2.33-eV laser excitations.[19–21] The Raman emission was analyzed by a spectrometer equipped with a CCD camera with a resolution of 2 cm^{-1}.[28]

Figure 2 shows typical electron-diffraction patterns and RBM Raman spectra for three SWNTs. From the electron-diffraction patterns [Figs. 2(a)–2(c), we determine these nanotubes to be (16,11), (25,12), and (33,23) SWNTs. Corresponding nanotube diameters can be obtained accurately from the chiral indices, and they are 1.84, 2.56, and 3.82 nm, respectively. For the three nanotubes we were able to obtain strong resonant Raman spectra of the RBM oscillations [Figs. 2(d)–2(f),[6] which yield their RBM frequencies at 124, 90, and 61 cm^{-1}. As one expects, larger diameter SWNTs have lower RBM oscillation frequencies.

Raman spectra of these nanotubes at larger Stokes shift covering the *D*-band and *G*-band phonons are shown in Figs. 3(a)–3(c). For the tangential *G*-mode vibration, we observed resonance frequencies at 1593, 1591, and 1589 cm^{-1}, similar to those of unstrained nanotubes on SiO_2/Si substrates.[3] It suggests that our suspended nanotubes have minimal built-in strain, because uniaxial strain is known to produce a downshift of *G*-mode frequency.[29] In all our SWNTs, the *D*-mode Raman peak is not observed. This absence of *D*-mode Raman peak shows that our suspended SWNTs are high quality with very low density of defects.

We obtained TEM diffraction data over 160 SWNTs, and 26 of these SWNTs have electronic transitions in resonance with our excitation lasers and show strong resonantly enhanced RBM Raman peaks. We summarize in Table I the combined electron-diffraction and Raman data of these 26 SWNTs. These nanotubes cover a large diameter range from 1.8 to 4.8 nm. It allows us to examine with high fidelity the diameter dependence of RBM oscillation frequencies. We plot in Fig. 4 the observed RBM frequency ω_{RBM} as a function of the inverse nanotube diameter $1/d$. The data can be perfectly described by a proportional relation by $\omega_{RBM} = A/d$ (cm^{-1} nm), where $A = 228 \pm 1$ (black line). It provides the directly experimental verification of the intrinsic $\omega_{RBM} - d$ scaling.

TABLE I. Chiral indices and RBM frequencies for 26 individual SWNTs.

Sample	(n, m)	d (nm)	ω_{RBM} (cm^{-1})
1	(16,11)	1.84	124.0
2	(23, 7)	2.13	107.0
3	(23, 7)	2.13	106.0
4	(25, 4)	2.13	105.5
5	(19,14)	2.25	101.5
6	(26, 5)	2.26	101.0
7	(25, 7)	2.28	102.0
8	(20,14)	2.32	99.0
9	(27, 6)	2.38	94.0
10	(27, 6)	2.38	94.0
11	(18,18)	2.44	94.0
12	(21,15)	2.45	95.0
13	(28, 6)	2.46	92.0
14	(25,12)	2.56	90.0
15	(21,17)	2.58	88.5
16	(32, 2)	2.59	88.0
17	(24,14)	2.61	87.5
18	(26,12)	2.63	84.5
19	(22,18)	2.72	85.0
20	(24,17)	2.79	83.0
21	(21,21)	2.85	80.0
22	(27,15)	2.89	78.0
23	(24,23)	3.19	72.0
24	(32,17)	3.37	67.0
25	(33,23)	3.82	61.0
26	(46,24)	4.82	48.0

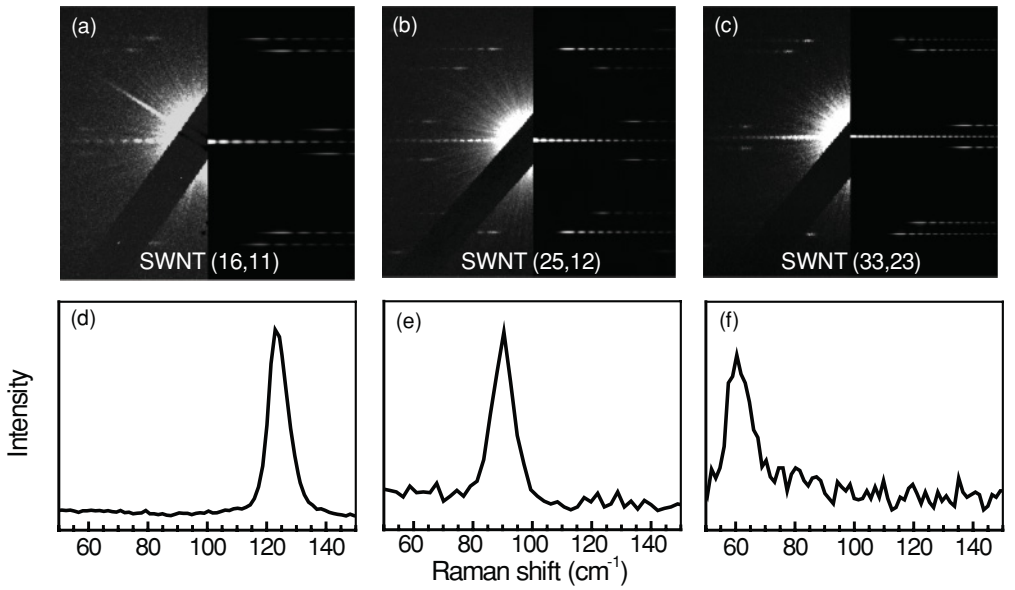

FIG. 2. Electron-diffraction patterns and RBM Raman spectra of three representative SWNTs. (a)–(c) Electron-diffraction patterns of the nanotube allow us to determine their chiral indices as (16,11), (25,12), and (33,23). The corresponding nanotube diameters are 1.84, 2.56, and 3.82 nm, respectively. (d)–(f) RBM Raman spectra of (16,11), (25,12), and (33,23) SWNTs. The RBM frequencies are located at 124, 90, and 61 cm^{-1}, respectively.

III. DISCUSSION

Our data further provide an accurate determination (with only 0.5% uncertainty) of the absolute A value, which relates directly to the force constants in graphitic structures. Because both the nanotube diameter and the Raman shift are measured in a direct fashion, our determination is free of systematic errors and can be used to test different theories. Many theoretical investigations of SWNT RBM oscillations exist in the literature. Jishi *et al.* used an empirical force constants method to predict the vibration frequencies.[12] Interaction up to fourth-nearest neighbor was considered, and the force constants were optimized to fit the experimental phonon dispersion of a flat graphene sheet, and they obtained a scaling factor A of 218. Kurti *et al.* carried out first-principles calculation to study the RBM oscillations of single-walled carbon nanotubes,[13] and found an A at 234. Other studies predicted a value of A between 222 and 252,[14] Our experimental value of 228 is quite close to that predicted by the first-principles calculation, but the theory still overestimates the oscillation frequency by about 2.5%. Using our value of A and treating SWNTs as continuous classic hollow cylinders, we estimate the graphene elastic constant at 28.8 ± 0.1 eV/Å^2. This might be the most accurate measure of graphene elastic constant so far.

We obtained the intrinsic behavior of RBM oscillations in SWNTs free from environmental perturbations by using clean, suspended nanotubes. Our results can be compared to the measured SWNT RBM oscillation frequencies when the nanotubes are interacting with the environment. Their difference can provide an estimate of environmental effects. For example, SWNTs in micelles suspended in water have RBM oscillations described by $\omega_{\mathrm{RBM}} = 223.5/d + 12.5$.[7] With the knowledge of intrinsic RBM oscillation behavior, we observe that the micelle-SWNT interactions modify both A and B values in the RBM frequency scaling, and they lead to a systematic blueshift of RBM frequencies in SWNTs.

IV. CONCLUSION

In summary, we have combined electron-diffraction and Raman-scattering techniques on the same suspended SWNTs to investigate the intrinsic behavior of RBM oscillations in

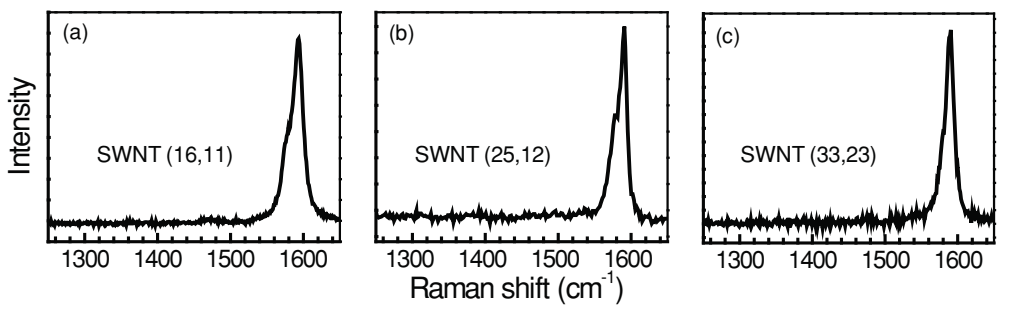

FIG. 3. Raman spectra covering the D-band and G-band region for (a) (16,11), (b) (25,12), and (c) (33,23) SWNTs. The D-mode Raman peak is not observed, indicating that our SWNTs are high quality with very few defects.

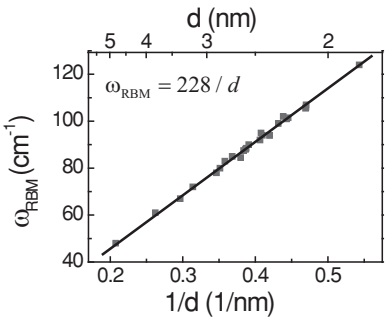

FIG. 4. RBM frequencies ω_{RBM} versus inverse nanotube diameters $1/d$ (squares). It is described perfectly by a proportional relation of $\omega_{RBM} = 228/d$ (cm^{-1} nm) (dark solid line).

carbon nanotubes. A prefect linear relation between RBM frequencies and inverse nanotube diameters was established. Understanding the intrinsic behavior of RBM oscillations not only is critical for spectral characterization of pristine SWNTs, but also opens up new opportunities for probing nanoscale coupling between SWNTs and other structures. One can envision that further controlled studies of RBM Raman in different environments will allow us to investigate quantitatively the interactions between SWNTs with adsorbed molecules, different solvents and surfactants, and with other nanotube species. Such studies can be combined with theoretical investigations to provide systematic understanding of physical interactions on the nanometer scale.

ACKNOWLEDGMENTS

This study was supported by NSF CAREER Grant No. 0846648, NSF Center for Integrated Nanomechanical Systems Grant No. EEC-0832819, and DOE Molecular Foundry Grant No. DE-AC02-05CH11231; and by the NSFC Grants No. 91021007, No. 10874218, No. 10974238, No. 20973195 and No. 50725209, and China MOST Grants No. 2009DFA01290 and No. 2007CB936203.

*egwang@pku.edu.cn
†fengwang76@berkeley.edu

[1] R. Saito, G. Dresselhaus, and M. S. Dresselhaus, *Physical Properties of Carbon Nanotubes* (Imperial College Press, London, 1998).
[2] S. Reich, C. Thomsen, and J. Maultzsch, *Carbon Nanotubes: Basic Concepts and Physical Properties* (Wiley-VCH, Weinheim, 2004).
[3] M. S. Dresselhaus, G. Dresselhaus, A. Jorio, A. G. Souza, and R. Saito, Carbon **40**, 2043 (2002).
[4] L. Alvarez, A. Righi, T. Guillard, S. Rols, E. Anglaret, D. Laplaze, and J. L. Sauvajol, Chem. Phys. Lett. **316**, 186 (2000).
[5] H. Kuzmany, W. Plank, M. Hulman, C. Kramberger, A. Gruneis, T. Pichler, H. Peterlik, H. Kataura, and Y. Achiba, Eur. Phys. J. B **22**, 307 (2001).
[6] A. Jorio, R. Saito, J. H. Hafner, C. M. Lieber, M. Hunter, T. McClure, G. Dresselhaus, and M. S. Dresselhaus, Phys. Rev. Lett. **86**, 1118 (2001).
[7] S. M. Bachilo, M. S. Strano, C. Kittrell, R. H. Hauge, R. E. Smalley, and R. B. Weisman, Science **298**, 2361 (2002).
[8] H. Telg, J. Maultzsch, S. Reich, F. Hennrich, and C. Thomsen, Phys. Rev. Lett. **93**, 177401 (2004).
[9] C. Fantini, A. Jorio, M. Souza, M. S. Strano, M. S. Dresselhaus, and M. A. Pimenta, Phys. Rev. Lett. **93**, 147406 (2004).
[10] P. T. Araujo, S. K. Doorn, S. Kilina, S. Tretiak, E. Einarsson, S. Maruyama, H. Chacham, M. A. Pimenta, and A. Jorio, Phys. Rev. Lett. **98**, 067401 (2007).
[11] P. T. Araujo, A. Jorio, M. S. Dresselhaus, K. Sato, and R. Saito, Phys. Rev. Lett. **103**, 146802 (2009).
[12] R. A. Jishi, L. Venkataraman, M. S. Dresselhaus, and G. Dresselhaus, Chem. Phys. Lett. **209**, 77 (1993).
[13] J. Kurti, G. Kresse, and H. Kuzmany, Phys. Rev. B **58**, R8869 (1998).
[14] G. D. Mahan, Phys. Rev. B **65**, 235402 (2002).
[15] P. T. Araujo, I. O. Maciel, P. B. C. Pesce, M. A. Pimenta, S. K. Doorn, H. Qian, A. Hartschuh, M. Steiner, L. Grigorian, K. Hata, and A. Jorio, Phys. Rev. B **77**, 241403 (2008).
[16] Z. J. Liu and L.-C. Qin, Chem. Phys. Lett. **408**, 75 (2005).
[17] H. Jiang, A. G. Nasibulin, D. P. Brown, and E. I. Kauppinen, Carbon **45**, 662 (2006).
[18] K. H. Liu, Z. Xu, W. L. Wang, P. Gao, W. Y. Fu, X. D. Bai, and E. G. Wang, J. Phys. D **42**, 125412 (2009).
[19] M. Y. Sfeir, F. Wang, L. M. Huang, C. C. Chuang, J. Hone, S. P. O'Brien, T. F. Heinz, and L. E. Brus, Science **306**, 1540 (2004).
[20] F. Wang, W. T. Liu, Y. Wu, M. Y. Sfeir, L. M. Huang, J. Hone, S. O'Brien, L. E. Brus, T. F. Heinz, and Y. R. Shen, Phys. Rev. Lett. **98**, 047402 (2007).
[21] S. Berciaud, C. Voisin, H Yan, B. Chandra, R. Caldwell, Y Shan, L. E. Brus, J. Hone, and T. F. Heinz, Phys. Rev. B **81**, 041414 (2010).
[22] H. Seidel, L. Csepregi, A. Heuberger, and H. Baumgartel, J. Electrochem. Soc. **137**, 3612 (1990).
[23] S. M. Huang, X. Y. Cai, and J. Liu, J. Am. Chem. Soc. **125**, 5636 (2003).
[24] A. J. Hart and A. H. Slocum, J. Phys. Chem. B **110**, 8250 (2006).
[25] X. S. Wang, Q. Q. Li, J. Xie, Z. Jin, J. Y. Wang, Y. Li, K. L. Jiang, and S. S. Fan, Nano. Lett. **9**, 3137 (2009).
[26] B. W. Smith and D. E. Luzzi, J. Appl. Phys. **90**, 3509 (2001).
[27] See supplemental material at [http://link.aps.org/supplemental/10.1103/PhysRevB.83.113404].
[28] A. G. Walsh, W. Bacsa, A. N. Vamivakas, and A. K. Swan, Nano. Lett. **8**, 4330 (2008).
[29] S. B. Cronin, A. K. Swan, M. S. Unlu, B. B. Goldberg, M. S. Dresselhaus, and M. Tinkham, Phys. Rev. Lett. **93**, 167401 (2004).